Food Hydrocolloids 126 (2022) 107459

Contents lists available at ScienceDirect

Food Hydrocolloids

journal homepage: www.elsevier.com/locate/foodhyd

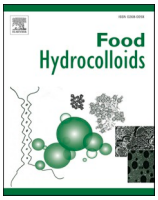

# Wheat starch-tannic acid complexes modulate physicochemical and rheological properties of wheat starch and its digestibility

Lijiao Kan [a], Edoardo Capuano [a,*], Teresa Oliviero [a], Stefano Renzetti [b]

[a] Food Quality and Design Group, Wageningen University and Research, Bornse Weilanden 9, 6708WG, Wageningen, the Netherlands
[b] Wageningen Food and Biobased Research, Wageningen University and Research, Bornse Weilanden 9, 6708WG, Wageningen, the Netherlands

ARTICLE INFO

*Keywords:*
Wheat starch
Tannic acid
Inclusion complexes
Non-inclusion complexes
Rheological properties

ABSTRACT

In this study, the interactions of wheat starch (WS) and tannic acid (TA) were investigated for their gelatinization, pasting, structural, rheological properties and digestibility of wheat starch. TA was either complexed with starch (WS-TA complexes) or mixed with starch (WS-TA mixtures) right before the characterization of its properties. The increase of melting enthalpy and temperature range ($T_{peak}$ - $T_{onset}$) associated with melting of amylose-lipid complex and the increase in the X-ray diffraction peak at $2\theta = 20^{\circ}$ possibly indicated the formation of inclusion types of complexes. The appearance of an endothermic transition at 130–160 °C indicated the formation of non-inclusion types of complexes. Non-inclusion type of complexes were mostly formed by co-gelatinization of WS-TA mixtures, while inclusion complexes would be mostly formed by complexation of TA with ungelatinized starch. TA in mixtures increased G′ and viscosity and decreased frequency dependency of the moduli, thus producing a stronger gel. TA in complexes decreased G′ and viscosity at low TA%, thus producing a weak gel, but increased gel strength at high TA%. The storage moduli G′ increased depending on the amount of TA involved in non-inclusion complexes. The formation of complexes between WS and TA largely slowed down the digestibility of gelatinized starch. The insights gained in this study provide opportunities to modulate starch techno-functional properties and digestibility in processing of starchy food.

## 1. Introduction

Starch acts as a thickening, gelling and texturizing ingredient in various processed food. Enrichment of starchy food such as bread and pasta with ingredients that contain polyphenols is of relevance for the food industry to develop healthy products (Kan, Oliviero, Verkerk, Fogliano, & Capuano, 2020; Oliviero & Fogliano, 2016). The addition of polyphenols can affect functional properties of starch, such as gelatinization, pasting properties and starch digestibility (M. Li, Pernell, & Ferruzzi, 2018). Understanding the mechanisms by which polyphenols affect the physicochemical properties of starch is gaining importance for food applications towards healthy diets (Gao et al., 2021).

The starch-polyphenols interactions has been recently investigated by producing starch-polyphenol complexes (Chi et al., 2017; Zheng et al., 2021) using methodologies such as ultrasound treatment, precipitation by adding an alcohol solution, and water-incubation of polyphenol-starch mixtures. Overall, incubation of a starch-polyphenol mixture in water for variable amounts of time is the preferred complexation method (Zhu, 2015). Association between starch and polyphenols can vary depending on conditions and source of starch and of polyphenols. One of the important complexes is V-type starch-phenolics complexes that are primarily driven by hydrophobic interactions (Zhu, 2015). In V-type complexes phenolics are hosted in the hydrophobic helical cavity of amylose (Biliaderis & Galloway, 1989). Evidence of V-type complexation have been shown with ferulic acid, gallic acid and green tea polyphenols, caffeic acid (Han, Bao, Wu, & Ouyang, 2020; Y.; Liu, Chen, Xu, Liang, & Zheng, 2019; Van Hung, Phat, & Phi, 2013; Zhao, Wang, Zheng, Chen, & Guo, 2019). Limiting factors for the formation of V-complexes are the bulky size, the lack of hydrophobicity of the phenolics, or the size of the cavity in the amylose helix (Zhu, 2015). In such cases some non-inclusion complexes were formed, which were mostly driven by hydrogen bonds (Zhu, 2015). The starch-polyphenols complexes have been extensively characterized by studying gelatinization, retrogradation, pasting and rheological properties and starch digestibility. Complexation with caffeic acid, gallic acid and ferulic acid significantly influenced rheological properties of potato and maize amylopectin, whereas digestibility of both types of starch was modestly slowed down by complexing with those three phenolic acids

* The corresponding author.
*E-mail address:* edoardo.capuano@wur.nl (E. Capuano).

https://doi.org/10.1016/j.foodhyd.2021.107459
Received 3 June 2021; Received in revised form 16 December 2021; Accepted 19 December 2021
Available online 22 December 2021

(Li et al., 2018). Complexing with quercetin enhanced crystallinity and compactness and clearly decreased starch digestibility of buckwheat starch (Gao et al., 2021). Although the interaction of a variety of polyphenols and starch has been widely reported, insufficient evidence was provided on the interacting mechanisms, for instance, by forming inclusion and non-inclusion complexes and corresponding forming conditions.

To expand the knowledge of starch-polyphenols interactions, the present study investigated the effect of addition of tannic acid (TA), a relatively less studied polyphenol, on wheat starch (WS) physicochemical properties and digestibility. To better understand the mechanisms of TA interaction with WS under different processing conditions, TA was added at different concentrations to WS in two ways, *i.e.,* by complexing or mixing with WS. WS-TA complexes were prepared by mixing and incubating native starch and tannins solutions and then washing out the unbound tannic acid. WS-TA mixtures were prepared by simply mixing native WS and TA just prior to starch characterization. The effect of TA on starch properties was investigated by characterizing starch crystallinity, swelling and pasting behaviour, starch gelatinization and the rheology of the resulting starch gels. These data were analysed against starch digestibility.

## 2. Materials and methodology

### 2.1. Materials

Wheat starch (moisture content 5%, lipids content <1%), tannic acid, pepsin (4268 units/mg), porcine pancreatin (P7545; 4XUSP specifications; amylase activity 40 units/mg), amyloglucosidase (P300 units/mL), bovine serum albumin (BSA), sodium dodecyl sulfate (SDS), 2-chloro-4-nitrophenyl-α-D-maltotrioside, triethanolamine (TEA) and ferric chloride were purchased from Sigma–Aldrich (St Louis, MO, USA). All other chemicals were of analytical grade.

### 2.2. Preparation of starch-tannins complex

The preparation of starch-tannins complex was performed according to a previous method with some modifications (Li et al., 2018). Ten gram of wheat starch (moisture content 5%) was mixed with amounts of tannic acid corresponding to 0%, 5%, 10% and 20% of starch dry weight. Then the mixed samples were dispersed in 250 mL of water. The mixture was put in a water bath of 37 °C for 30 min and the suspension was stirred every 5 min. Then it was centrifuged at 3500 g for 10 min. The supernatant was stored for analysis of tannins content, the resulting precipitates were washed with distilled water until no tannins was detected in the supernatant. The whole of the washing solution was collected for measuring free tannic acid content as described in section 2.3. Then the precipitation was freeze dried to obtain non-gelatinized starch-tannins complexes. According to the initial amount of TA (0%, 5%, 10% and 20%), the wheat starch-tannic acid complexes were marked as C0, C5, C10 and C20, respectively. The amount of TA added to starch is implicit in the sample coding, and C5, C10 and C20 is the starch-TA complex produced by adding 5%, 10 and 20% w/w TA to starch and removing the free TA. In addition, starch-tannins mixtures in this study were prepared by simply mixing native starch with tannic acid which dissolved in water just before the starch characterization. According to the initial amount of TA (0%, 5%, 10% and 20%) to be mixed with wheat starch, the wheat starch-tannic acid mixtures were marked as M0, M5, M10 and M20, respectively.

### 2.3. Quantification of bound tannins

The determination of tannins was performed using a BSA precipitation method according to our previous paper (Kan, Capuano, Fogliano, Oliviero, & Verkerk, 2020). This determination has been done only on WS-TA complexes. The bound tannins were calculated by the initial amount of tannins minus the free tannins. The free tannins were defined as the tannic acid which was released in the supernatant upon preparation of starch-tannins complex as described in 2.2.

### 2.4. Determination apparent amylose

Amylose content was estimated by iodine colorimetry according to (H. Li et al., 2019) with slight modifications. This determination has been done only on native wheat starch and wheat starch-tannic acid complexes. A standard curve with amylose content ranging from 0 to 100% was prepared using pure potato amylose (Sigma A0512) and maize amylopectin (Sigma 10120). Native wheat starch, wheat starch-tannic acid complexes, amylose and amylopectin were suspended in 1 M aqueous NaOH (10 mg/mL), followed by heating in a boiling water bath with shaking. After cooling down to room temperature and five-times dilution in water, a 40 μL aliquot was added into 1 mL water in a 2 mL Eppendorf tube, followed by adding 200 μL iodine solution (0.0025 M $I_2$/0.0065 M KI mixture) and 760 μL water to make up 2 mL solution. The solution was mixed vigorously and then allowed to develop color for 15 min. The absorbance was read at 600 nm. A standard starch (labelled as 68% amylose content) of K-AMYL Kit (Megazyme, Ireland) tested with the iodometric assay as reference gave 66.4 ± 0.6% amylose content at 600 nm. The moisture content of all starches was determined for the calculation of amylose content on a dry weight basis.

### 2.5. Determination of amylose leaching, swelling power and solubility

Amylose leaching, swelling factor and solubility were determined according to a previous method with some modifications (Guo, Zhao, Chen, Chen, & Zheng, 2019). Briefly, 1 g of wheat starch-tannic acid complexes prepared in 2.2 was mixed with 25 mL of water. For the mixture samples, 1 g of wheat starch (dry weight basis) was mixed with 0, 50, 100, 200 mg of tannic acid, and then 25 mL of water was added. Then the starch suspensions were put in a boiled water-bath for 30 min. After cooling down to room temperature, all the samples was centrifuged at 3500 g for 10 min. Leached amylose content in the supernatant was determined by the above-mentioned iodine binding technique. The supernatant and pellet were dried at 105 °C overnight. The dried supernatant and the water in swollen granules were weighed. The solubility was defined as the ratio of the weight of dried supernatant to the weight of starch samples (g/100g). The swelling power was defined as the ratio of the wet weight of the pellet to the dry weight of starch (g/g).

### 2.6. DSC analysis

The melting behaviour of crystalline structures in starch-tannins complex samples and mixture samples was determined by a Q 200 differential scanning calorimeter (TA Instruments, New Castle, DE, USA) (Bin Zhang, Huang, Luo, & Fu, 2012). Regarding the starch-tannins complexes, 7.5 mg of freeze dried starch-tannins complexes were placed in high-volume, high-pressure aluminium pans. Then, 22.5 mL of demineralized water were added. Regarding the wheat starch-tannic acid mixtures, 7.5 mg of wheat starch was placed in high-volume, high-pressure aluminium pans, and then 22.5 mL of tannic acid solutions was added. For providing 0%, 5%, 10% and 20% of wheat starch (based on 7.5 mg), the concentrations of tannic acid were 0, 0.017, 0.033, 0.066 mg/mL, respectively. All the samples in pans were kept overnight to equilibrate and this step was used to make sure all the powder samples would be well hydrated. Upon start, the samples were held at 5 °C for 5 min, then scanned from 5 °C to 160 °C at 5 °C/min. Then a cooling cycle was performed from 160 to 40 °C at 5 °C/min. Finally, a 2nd scan was performed from 40 °C to 160 °C. Onset ($T_{onset}$), peak ($T_{peak}$) and conclusion ($T_{conclusion}$) temperatures, as well as the enthalpy were determined. Analysis was done with TA Instruments Universal Analysis 2000 software, version 4.5A, build 4.5.0.5 (TA

Instruments, New Castle, DE, USA).

### 2.7. XRD analysis

The X-ray diffraction (XRD) experiments were performed using an X-ray diffractometer (D8 Advance, Bruker Inc., Germany) with the 2θ (°) range of 5-55° (Zhang, Li, Liu, Xie, & Chen, 2013). Native wheat starch and wheat starch-tannic acid complexes prepared in section 2.2 were directly analysed by XRD. Gelatinization of wheat starch-tannic acid complexes and mixtures were performed according to section 2.5. After cooling down to room temperature, the samples were dried in a freeze dryer (Alpha 2–4 LD plus, Christ). Then the gelatinized wheat-starch-tannic acid complexes and mixtures were analysed by XRD. The relative crystallinity (RC) was quantitatively estimated as a ratio of the crystalline area of the total area (crystalline regions plus amorphous regions) using Diffrac.eva.V5.2 software.

### 2.8. RVA analysis

Pasting behaviour was investigated using a Rapid Visco Analyser Super 4 (Perten, Hägersten, Sweden), according to a previous method with slight modifications (S. Liu, Yuan, et al., 2019). Regarding the starch-tannin complexes, inside a suitable canister 3.00 ± 0.01 g of wheat starch-tannic acid complexes (dry basis) is mixed manually with 22.0 g ± 0.1 g of distilled water until no lumps were visual anymore. Regarding the wheat starch-tannic acid mixtures, 0.15, 0.3, 0.6 g of tannic acid was added into 22.0 g ± 0.1 g of distilled water, then 3.00 ± 0.01 g of wheat starch was added. The experiment was started with an initial stirring speed of 960 rpm at 50 °C for 60 s. Then, the stirring speed is decreased to 160 rpm while the temperature is increased to 95 °C within 3 min 42 s. Hold at 95 °C for 2 min 30 s min. Then cool to 50 °C within 3 min 48 s and hold at 50 °C for 4 min.

### 2.9. Small amplitude oscillatory rheology of starch-tannic acid gels

Wheat starch suspensions (5%, *w/v*) were prepared. Briefly, 1.25 g of wheat starch-tannic acid complexes (dry weight basis of starch) was dispersed in 23.75 g of water. Wheat starch-tannic acid mixtures were simply prepared by mixing 1.25 g of wheat starch (dry weight basis) with 62.5, 125 and 250 mg of tannic acid and then 23.75 g of water was added. The starch gelatinization was done using RVA as described in 2.8. The samples were left at room temperature for 1 h to reach 25 °C. Then the rheological properties of the gelatinized samples were evaluated.

Dynamic viscoelastic properties of gels were determined using a rotary rheometer (Discovery, HR-3, TA instrument Inc., USA) equipped with a parallel plate geometry (40 mm) at 1.0 mm gap. Amplitude sweep experiment tests were conducted to record the storage modulus (G′) and loss modulus (G″) as function of a strain from 0.01 to 1000%. Frequency was set at 1 Hz. Frequency sweeps tests were performed at an angular frequency range of 1–100 rad/s$^{-1}$ with a strain of 1%, which was within the linear visco-elastic region (as determined by the amplitude sweeps). The frequency sweep data were fitted with a power law model as shown below.

$$G' = k' \times w^{n'} \quad (1)$$

where $w$ is the oscillation frequency, and $k'$ is model constants. The constant $n'$ is the slope in a log–log plot of $G'$ versus $w$.

The steady shear flow behavior was conducted using the same rheometer set. Viscous flow behavior was obtained at strain-controlled mode with shear rates going from of 0.1–100 s$^{-1}$.

### 2.10. In vitro digestibility

A standard *in vitro* simulated process was used in this study which was modified for the amount of α-amylase (Minekus et al., 2014). Four different sets of samples were prepared for the *in vitro* digestion experiments: 1) Wheat starch-tannic acid complexes (C0, C5, C10 and C20 prepared in section 2.2) were directly used for *in vitro* digestion. 2) Wheat starch-tannic acid mixtures were prepared by simply mixing 2.5 g of native wheat starch with 0.125, 0.25 and 0.5 g of tannic acid. 3) & 4) Gelatinized wheat starch-tannic acid complexes and mixtures were prepared according to section 2.5. After cooling down to room temperature, they were freeze dried and used for digestion experiments and resistant starch measurement. The resistant starch content was measured by the Resistant Starch Assay Kit (Megazyme).

Briefly, 2.5 g of the samples was mixed with 2.5 g of water for hydration. Then the samples were treated with simulated gastric fluids and pepsin (5.86 mg/mL, the pepsin activity is 4268 U/mg). The pH of the mixture was adjusted to 3 and incubated at 37 °C with agitation for 2 h. Then, simulated intestinal fluids and pancreatin (40 mg/mL, the α-amylase activity is 40 U/mg) were added to the mixture and the pH was adjusted to 7. The mixture was incubated at 37 °C with agitation for 2 h. During the intestinal phase, 0.1 mL of sample was collected at different time points (0, 10, 20, 40, 60,80, 100, 120 min). Then 0.4 mL of absolute ethanol was added to stop the reaction and the mixture was centrifuged at 13000 g for 10 min. Finally, 2 mL of amyloglucosidase (27.16 U/mL) was added and incubated at 37 °C for an extra hour to complete starch digestion. The bio-accessibility of TA after gastric digestion was measured according to our recently published paper (Kan, Capuano, et al., 2020). A first-order kinetics model was applied to describe the kinetics of glucose release from starch digestion (Dona, Pages, Gilbert, & Kuchel, 2010).

$$C_t - C_0 = C_\infty\left(1 - e^{-kt}\right). \quad (2)$$

where $C_t$, $C_0$ and $C_\infty$ correspond to the percentage of digested starch at time t, 0 and infinite time, and $k$ is the kinetic constant. Parameter estimation was performed using the solver function of excel software by minimizing the residual sum of square values.

### 2.11. α-amylase inhibition by tannic acid in wheat starch-tannins complexes and mixtures

The α-amylase inhibition assay was conducted according to a previous method with some modifications (Okutan, Kongstad, Jäger, & Staerk, 2014). Briefly, 50 mg of porcine pancreatic α-amylase (10 units/mg, Sigma St. Louis, MO, USA) was dissolved in 10 mL of 100 mmol phosphate buffer (pH 7.0) containing 2 mg/mL bovine serum albumin and used as an enzyme solution. One hundred μM 2-Chloro-4-nitrophenyl-α-D-maltotrioside was dissolved in the same buffer (pH 7.0) and used as substrate solution. The α-amylase inhibition of free and bound tannic acid were tested separately. Free tannic acid referred to the tannins that either potentially released from the wheat starch-tannic acid complexes, or did not interacted with starch in the wheat starch-tannins mixtures. For free tannic acid: 50 μL of enzyme solution and 10 μL of phosphate buffer (control) or different concentrations of tannic acid were mixed in a well of a microplate reader. After incubation for 5 min, substrate solution (50 μL) was added and incubated for another 5 min at room temperature. The absorbance at 405 nm was measured using a microplate reader. Bound tannic acid referred to the tannins that bound to wheat starch. For the bound tannic acid: 100 mg of wheat starch-tannins complex (sample C20, prepared in section 2.2) was mixed with 1 mL of enzyme solution. The mixture was incubated for 5 min at room temperature. Then the mixture was centrifuged (4500 g, 5 min). Then 60 μL of the supernatant was mixed with 50 μL of substrate. The remaining steps were the same as free tannic acid. The inhibition on α-amylase was calculated by the following equation:

$$\text{Inhibition } (\%) = \left(A_{\text{control}} - A_{\text{sample}}\right) / A_{\text{control}} * 100$$

For free tannic acid: A $_{\text{control}}$ is the absorbance of mixture of phosphate buffer, enzyme and substrate; A $_{\text{sample}}$ is the absorbance of mixture

of tannic acid, enzyme and substrate; For bound tannic acid: $A_{control}$ is the absorbance of mixture of supernatant from complex control (C0), enzyme and substrate. $A_{sample}$ is the absorbance of mixture of supernatant from sample C20, enzyme and substrate.

### 2.12. Statistics

The results were expressed as mean ± standard deviation (SD). One-way analysis of variance (ANOVA) followed by the Duncan's multiple range test was used to compare the means among different groups by the SAS 9.4 (SAS Institute Inc., Cary, NC, USA). Differences were considered significant at $p < 0.05$.

## 3. Results

### 3.1. Swelling power and amylose leaching

In our study, WS-TA (wheat starch-tannic acid) complexes were prepared by mixing WS with different amount of TA for a certain time and removing free TA. As shown in Table 1, 22.6, 40.9 and 68.4 mg/g of complexed TA was detected when wheat starch was complexed with 5, 10 and 20% tannic acid on dry weight of starch, respectively. An equilibrium seemed to be reached among complexed and free TA, since 30–40% of the added TA complexed with WS and was not collected in the washing out water after incubation. The effect of those complexed TA on apparent amylose content, swelling power and solubility was investigated. As shown in Table 1, a significant increase of the content of apparent amylose was observed in WS-TA complexes, *e.g.*, from 33.0% (C0) to 46.0% (C20). In line with the increased amount of apparent amylose, the amylose leaching also significantly increased *e.g.,* from 14.3 (C0) to 16.8 g/100g (C5), independently from the amount of bound TA. The swelling power and solubility also significantly increased when WS was complexed with different amount of TA. Mixed TA showed opposite effects on amylose leaching of WS, *i.e.* mixed TA reduced the amylose leaching of WS and the reduction significantly increased with increasing amount of TA added. The solubility and swelling power of M5 and M10 was higher than native starch, but decreased significantly in M20. It was noted that the swelling power and amylose leaching of the C0 control was higher than M0, *i.e.* the native WS.

TA in complexes and mixtures also showed clear differences in pasting behaviours as shown in Table S1 and Fig. S1. For instance, TA in mixtures caused a progressive reduction in peak viscosity, whereas TA in complexes caused limited reduction in peak viscosity, independently with the amount of TA.

**Table 1**
The amount of tannic acid bound to starch, apparent amylose, amylose leaching, solubility and swelling power of wheat starch by complexation or mixing with tannic acid.

| | Bound tannic acid mg/g DW of non-gelatinized complex | Apparent amylose (g/100 g DW of starch) | Amylose leaching (g/100 g DW of starch) | Solubility (g/100 g DW of starch) | Swelling power (g/g DW of starch) |
|---|---|---|---|---|---|
| C0 | 0 | 33.0 ± 0.8 a | 14.3 ± 0.2 d | 20.0 ± 0.0 e | 13.9 ± 0.1 e |
| C5 | 22.6 ± 1.4 a | 33.4 ± 0.2 ab | 16.8 ± 0.2 e | 21.1 ± 0.5 f | 15.4 ± 0.2 gh |
| C10 | 40.9 ± 0.1 b | 36.0 ± 0.1 c | 16.8 ± 0.21 e | 22.1 ± 1.1 fg | 15.2 ± 0.2 fg |
| C20 | 68.4 ± 1.6 c | 46.0 ± 0.4 d | 16.7 ± 0.4 e | 23.1 ± 1.6 gh | 15.0 ± 0.1 f |
| M0 | na | 33.5 ± 0.9 a | 14.5 ± 0.2 d | 16.0 ± 0.0 b | 11.2 ± 0.2 b |
| M5 | na | na | 12.6 ± 0.2 c | 16.5 ± 0.0 d | 11.8 ± 0.2 c |
| M10 | na | na | 11.8 ± 0.1 b | 16.2 ± 0.1 c | 12.4 ± 0.4 d |
| M20 | na | na | 5.4 ± 0.0 a | 15.0 ± 0.0 a | 9.1 ± 0.1 a |

C0, C5, C10 and C20 were starch-tannins complexes with increasing amount of bound TA. The amount of TA added to starch is implicit in the sample coding, so C5, C10 and C20 is the starch-TA complex produced by adding 5%, 10 and 20% w/w TA to starch and removing the free TA.
M0, M5, M10 and M20 were starch-tannins mixtures in this study, which were prepared by simply mixing native starch with 0%, 5%, 10% and 20% of tannic acid (dry weight basis of starch) just prior to amylose leaching, solubility and swelling power analysis. M0 represents NWS (native wheat starch).The amount of TA in the mixtures is much higher than that in complex samples.
na: not applicable.
Results are expressed as mean ± standard deviation of triplicates. Different letters in the same column indicate a.
significant difference between means ($p < 0.05$).
WS, wheat starch; TA, tannic acid.

### 3.2. DSC

As shown in Fig. 1 and Table 2, the first endothermic transition appeared at around 60 °C and was associated with melting of the crystalline amylopectin structures. Both complexed and mixed TA facilitated the gelatinization of wheat starch with lower gelatinization temperatures. Complexed TA and 5% and 10% mixed TA caused no change on enthalpy of melting, whereas 20% mixed TA caused a lower enthalpy of melting. The second endothermic transition that appeared at around 100 °C was associated with the melting of the amylose-lipid complex. Both complexed and mixed TA caused a lower melting temperature and higher temperature range ($T_{peak}$ - $T_{onset}$), as well as the higher enthalpy of melting of the amylose-lipid complex. In addition, melting enthalpy and temperature range ($T_{peak}$ - $T_{onset}$) of amylose-lipid complex was higher in WS-TA complexes than in WS-TA mixtures. During the cooling stage after the initial heating, all samples displayed one exothermic transition, which were attributed to the formation of starch−lipid complex (Supplementary Table S2). A third endothermic transition at 130–150 °C appeared only for samples C10, C20 and M5-M20, which was associated with the formation of amylose-tannins complexes. As shown in Fig. 1, only a small peak appeared in C10 and C20, but much larger peaks appeared in WS-TA mixtures. The enthalpy of this transition increased with the amount of TA complexed or mixed with starch (Fig. 1 A&C). This peak was not thermo-reversible since it did not appear in the reheating cycle (Fig. 1 B&D) and during cooling stage (Table S2).

### 3.3. XRD

The XRD patterns and corresponding crystallinity of native wheat starch, WS-TA complexes, gelatinized WS-TA complexes and gelatinized WS-TA mixtures are shown in Fig. 2. As shown in Fig. 2A, native WS presented a typical A-type XRD pattern with strong peaks at $2\theta = 15°$, 17°, 18° and 23°, and this is generally regarded as the typical A-type starch (Pan et al., 2019). Complexed TA increased the relative crystallinity (RC) of wheat starch, *e.g.*, C0 and C1 complex showed a RC value of 33.9% and 36.5%, respectively. The XRD patterns of gelatinized WS-TA complexes and gelatinized WS-TA mixtures were measured and shown in Fig. 2 C&D. The RC of gelatinized starch increased dependently with the amount of complexed and mixed TA (Fig. 2 C&D). The relative increase in RC was much higher for complexes than for mixtures in the gelatinized samples.

### 3.4. Rheological properties

#### 3.4.1. Frequency sweep

The frequency dependence of the elastic and viscous moduli (*i.e.* G′ and G″, respectively) from all WS gels in the study is shown in Fig. 3. The G′ exceeded G″ without any crossover point within the frequency range of 0.01–100 rad/s in all the samples except for the native wheat starch (M0) and for C5. A clear crossover point where G′ equals G″ was found in

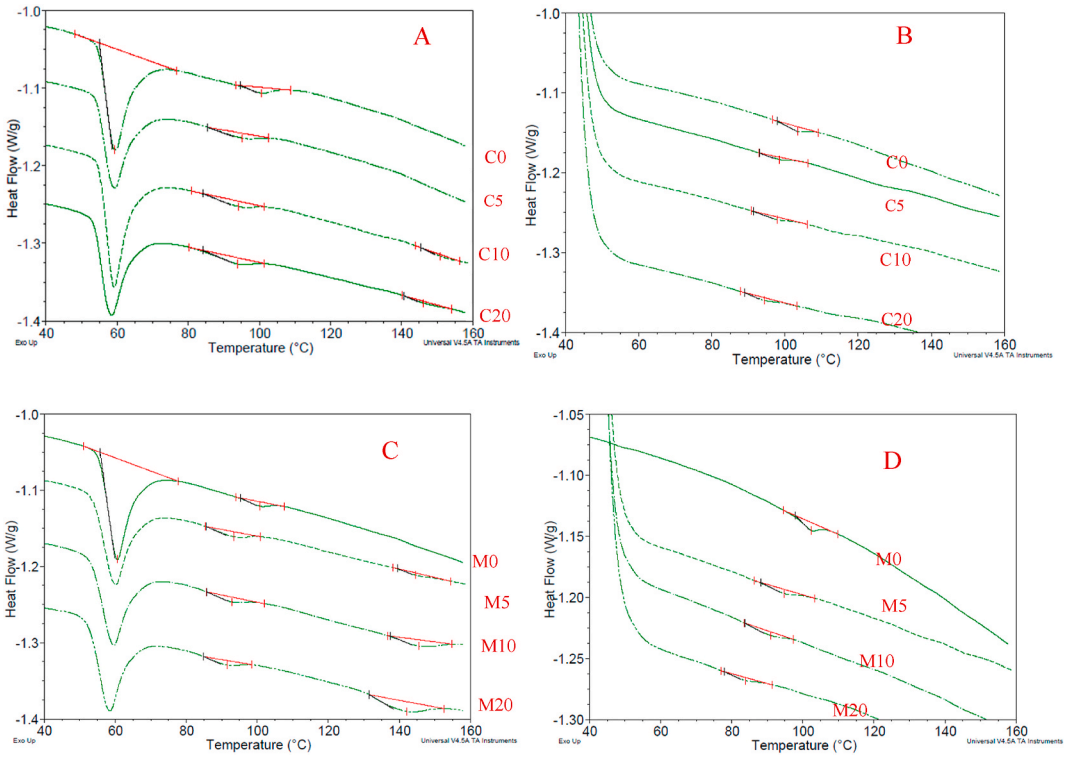


**Fig. 1.** Thermal behaviour curve of: A) First cycle of wheat starch complexed with 5%, 10% and 20% of tannic acid; B) Second cycle of wheat starch complexed with 5%, 10% and 20% of tannic acid; C) First cycle of wheat starch mixed with 5%, 10% and 20% of tannic acid. D) Second cycle of wheat starch mixed with 5%, 10% and 20% of tannic acid. C0, C5, C10 and C20 is the starch-TA complex produced by adding 0%, 5%, 10% and 20% w/w TA to starch and removing the free TA. M5, M10 and M20 were starch-tannins mixtures in this study, which were prepared by simply mixing native starch with 5%, 10% and 20% of tannic acid (dry weight basis of starch). M0 represents NWS (native wheat starch).

M0 and C5 at around 50 rad/s as marked at Fig. 3A and C, respectively, after which G″ started to exceed G′. The power-law model was fitted at the frequency range where G′ was higher than G″. The power-law model's parameters are presented in Table 3. Complexed TA and mixed TA showed different trends for the power-law model's parameters. Smaller amount of TA in complexes (*i.e.* C5 and C10) significantly lowered the $k$' and $k$" values and increased the $n$' and $n$'' values. Large amount of TA in complexes (*i.e.* C20) significantly increased the $k$' and $k$" values and decreased the $n$' and $n$'' values. However, TA in mixtures caused a significant increase of $k$' and $k$" values and significant reduction of $n$' and $n$'' values, though the increase and reduction is not always TA-dose dependent.

### 3.4.2. Amplitude sweep

From the results of amplitude experiments (Fig. 4), two distinct domains including linear viscoelastic (LVE) and non-linear viscoelastic regions were attained. In the LVE region, the G′ and G″ were almost constant and in the non-linear region both started to sharply decrease. A strain hardening behaviour was found as indicated by the small peak in G′ and G″ (Fig. 4). In agreement with the transient network theory, strain hardening evidence a shear-induced increase of the density of elastically active chains through an increase in the proportion of bridging chains (Brassinne, Gohy, & Fustin, 2014). The rheological parameters are shown in Table 3. The storage moduli in the LVE region (i.e. $G'_{LVE}$) were higher than the loss moduli (i.e. $G''_{LVE}$) for all samples. Compared to the control C0, C5 and C10 showed a decrease in $G'_{LVE}$ and $G''_{LVE}$, while a significant increase was observed for C20. Compared to M0, $G'_{LVE}$ and $G''_{LVE}$ of M5, M10 and M20 significantly increased with increasing amount of TA added.

### 3.4.3. Steady flow properties

The flow behaviour of WS-TA complexes and mixtures is shown in Fig. S2. The viscosity of all starch pastes decreases exponentially with increasing the shear rate. C5 showed lower viscosity than complex control (C0) while C10 and C20 showed higher viscosity (Fig. S2). The starch mixed with TA exhibited higher apparent viscosity than M0 predominantly in the lower shear rate, i.e. 0.01–1 1/s (Fig. S2).

### 3.5. In vitro digestibility

The effect of TA on starch digestibility was investigated in WS-TA complexes and mixtures (Fig. 5). A limited exponential model was fitted to the data and the estimated $k$ and $C_\infty$ are shown in Table 4. Within the ungelatinized WS-TA complexes, only C10 and C20 showed a significant inhibition of starch digestion, *i.e.,*26.9% and 3.4% of starch was digested (Fig. 5A and Table 4). The WS-TA complexes were then gelatinized and the starch digestibility was measured (Fig. 5C). The starch digestibility of all the gelatinized complexes was decreased compared to the native starch and a clear dose-dependent inhibition by complexed TA was observed. Starch-tannins mixtures were also prepared by simply mixing native starch with tannic acid just prior to "*in vitro* digestion" and "gelatinization and *in vitro* digestion" as shown in Fig. 5B&D, respectively. For both non-gelatinized and gelatinized starch, the starch digestibility was significantly inhibited by 5% of mixed TA. Remarkably, 10% and 20% of mixed almost inhibited all the starch digestibility (Fig. 5B&D). The size of inhibition for mixed TA was much larger than for complexed TA for the gelatinized samples as indicated by the resistant starch (RS) content which was measured (Table 4). For the non-gelatinized WS-TA complex, more than 70% of RS was detected compared to the control C0 (i.e. 1.73%). Similar results were observed all the gelatinized samples (Table 4), *i.e.*, 40%~60% of RS was found in gelatinized WS-TA complex and mixtures, whereas about 6% of RS was found in C0 and M0.

**Table 2**
The effect of tannic acid on the gelatinization starch by thermal analysis using differential scanning calorimeter.

| 1st peak | $T_{onset}$ (°C) | $T_{peak}$ (°C) | $T_{conclusion}$ (°C) | Δ $T_{peak}$- $T_{onset}$ (°C) | Enthalpy (J/g) |
|---|---|---|---|---|---|
| C0 | 54.6 ± 0.3 d | 59.0 ± 0.2 bc | 65.7 ± 0.4 bc | 4.4 ± 0.1 a | 12.0 ± 0.4 b |
| C5 | 54.2 ± 0.1 bcd | 58.9 ± 0.2 bc | 65.4 ± 0.2 ab | 4.7 ± 0.1 ab | 12.3 ± 0.1 b |
| C10 | 54.0 ± 0.2 bc | 58.6 ± 0.1 ab | 65.2 ± 0.3 ab | 4.6 ± 0.1 ab | 12.4 ± 0.3 b |
| C20 | 53.7 ± 0.1 b | 58.4 ± 0.1 a | 64.8 ± 0.1 ab | 4.7 ± 0.0 ab | 12.5 ± 0.3 b |
| M0 | 55.6 ± 0.1 e | 60.6 ± 0.1 e | 67.2 ± 0.3 d | 4.9 ± 0.2 b | 12.2 ± 0.4 b |
| M5 | 54.5 ± 0.0 cd | 60.0 ± 0.0 d | 66.6 ± 0.3 cd | 5.5 ± 0.0 c | 12.0 ± 0.1 b |
| M10 | 53.8 ± 0.1 b | 59.3 ± 0.1 c | 65.7 ± 0.1 bc | 5.5 ± 0.2 c | 11.6 ± 0.3 ab |
| M20 | 52.9 ± 0.1a | 58.4 ± 0.1 a | 64.6 ± 0.3 a | 5.5 ± 0.1 c | 11.0 ± 0.1 a |
| **2nd peak** | Tonset (°C) | Tpeak (°C) | Tconclusion (°C) | Δ Tpeak-Tonset (°C) | Enthalpy (J/g) |
| C0 | 94.3 ± 0.6 d | 100.5 ± 0.2 e | 105.6 ± 0.3 d | 6.2 ± 0.4 ab | 0.59 ± 0.04 b |
| C5 | 85.8 ± 0.3 bc | 95.1 ± 0.2 d | 101.4 ± 0.4 c | 9.4 ± 0.3 d | 0.71 ± 0.08 b |
| C10 | 84.0 ± 0.3 ab | 94.0 ± 0.1 c | 100.8 ± 0.9 bc | 10.0 ± 0.3 de | 0.89 ± 0.02 c |
| C20 | 82.4 ± 0.4 a | 93.1 ± 0.7 bc | 99.9 ± 0.5 bc | 10.8 ± 0.4 e | 1.08 ± 0.10 d |
| M0 | 95.2 ± 0.1 d | 100.6 ± 0.1 e | 106.2 ± 0.2 d | 5.4 ± 0.1 a | 0.42 ± 0.03 a |
| M5 | 86.0 ± 1.0 c | 93.6 ± 0.4 c | 99.8 ± 0.7 bc | 7.6 ± 0.7 c | 0.61 ± 0.09 b |
| M10 | 85.5 ± 0.8 bc | 92.3 ± 0.2 ab | 99.0 ± 0.6 ab | 6.8 ± 1.0 bc | 0.64 ± 0.09 b |
| M20 | 84.7 ± 0.4 bc | 91.7 ± 0.2 a | 97.8 ± 0.4 a | 7.0 ± 0.1 bc | 0.61 ± 0.02 b |
| **3rd peak** | Tonset (°C) | Tpeak (°C) | Tconclusion (°C) | Δ Tpeak-Tonset (°C) | Enthalpy (J/g) |
| C0 | nd | nd | nd | nd | nd |
| C5 | nd | nd | nd | nd | nd |
| C10 | 145. 8 ± 0.0 c | 151.3 ± 0.0 c | 145. 8 ± 0.0 bc | 5.5 ± 0.0 a | 0.21 ± 0.02 a |
| C20 | 140.5 ± 0.1 b | 145.2 ± 0.1 b | 140.5 ± 0.1 a | 4.7 ± 0.1 a | 0.24 ± 0.08 a |
| M0 | nd | nd | nd | nd | nd |
| M5 | 141.1 ± 0.0 b | 151.5 ± 0.0 c | 155.3 ± 0.0 c | 10.4 ± 0.0 c | 0.89 ± 0.00 b |
| M10 | 138.5 ± 2.6 b | 146.6 ± 1.5 b | 153.2 ± 1.6 b | 8.1 ± 1.1 b | 1.04 ± 0.08 b |
| M20 | 131.5 ± 1.0 a | 142.5 ± 0.6 a | 150.2 ± 0.3 a | 11.0 ± 0.5 c | 1.88 ± 0.34 c |

1st peak represents starch gelatinization, 2nd peak represents inclusion starch-lipid/tannic acid complexes, 3rd peak represents non-inclusion starch-tannic acid complexes$T_{onset}$ temperature, it defines the start of the peak. $T_{peak}$ temperature, it defines the temperature that causes the largest heat flow difference. $T_{conclusion}$ temperature, it defines the end of the peak. Enthalpy shows the melting enthalpy, indicating the amount of energy required to melt the starch granules. All temperatures are expressed in °C. nd; not detected.Results are expressed as mean ± standard deviation of triplicate. Different letters in the same column indicate significant difference. pH of C0, C5, C10 and C20 were 7.0, 4.7, 4.6 and 4.2, respectively. pH of M0, M5 TA, M10 and M20 were 7, 4.6, 3.4 and 3.3, respectively.C0, C5, C10 and C20 is the starch-TA complex produced by adding 0%, 5%, 10% and 20% w/w TA to starch and removing the free TA. M5, M10 and M20 were starch-tannins mixtures in this study, which were prepared by simply mixing native starch with 5%, 10% and 20% of tannic acid (dry weight basis of starch). M0 represents NWS (native wheat starch).

## 4. Discussion

Starch and phenolic compounds were reported to form either V-types inclusion complexes with amylose single helices facilitated by hydrophobic interactions, or non-inclusion complexes with much weaker binding mostly through hydrogen bonds (Chai, Wang, & Zhang, 2013). Monomeric phenolics and condensed tannins have both been reported to interact with starch to modify its physiochemical properties (Amoako & Awika, 2016; Gao et al., 2021). TA, which belongs to the class of hydrolysable tannins was rarely studied for interaction with starch. Besides, most of the studies focused on V-type inclusion complexes, whereas non-inclusion complexes were not widely reported. Against this background, our study aimed to modulate the interaction between TA and wheat starch and gain insights in the underlying mechanisms. For such purpose, TA was added to starch either by a complexation procedure (WS-TA complexes) or as solute to a suspension of starch in water (WS-TA mixtures).

Differences between WS-TA complexes and mixtures were driven by the stage at which TA interacted with starch and by the amount of TA which effectively interacted. Under the conditions used to prepare the WS-TA complexes (*i.e.* co-incubating of WS with TA at 37 °C for 0.5 h), TA had more time to interact with starch and more importantly, it only interacted with native starch. During the preparation of mixtures, TA likely interacted with starch while granules were swelling and gelatinizing (Donald, 2001; Waigh, Gidley, Komanshek, & Donald, 2000) and had less time to interact with the native starch. The range of TA concentrations interacting with starch during gelatinization was larger in the mixtures than in the complexes, although they partially overlapped. The free TA which did not bind to native starch during incubation was removed when preparing WS-TA complexes. Additionally, it should be noted that the incubation procedure also affected the properties of the native starch. In fact, the control sample for the WS-TA complexes (i.e. C0), showed different characteristics compared with the native wheat starch (i.e. M0) (Tables 1–4 and Figs. 1–4). Possibly, during incubation in water without TA, starch hydration and swelling caused a transition from nematic structure to smectic structure, thus altering its properties compared to the native wheat starch (Donald, 2001; Renzetti, van den Hoek, & van der Sman, 2021).

Complexation of TA with WS by incubation at 37 °C for 30 min affected the apparent amylose content, swelling power, amylose leaching and pasting properties of wheat starch. During incubation, TA likely penetrated in the starch granules, interacting with the amorphous regions constituted of amylose and non-ordered amylopectin branches, resulting in higher swelling power and amylose leaching (Table 1). In contrast with previous observations (Blazek & Copeland, 2008), these changes were associated with a reduction in peak viscosity (Table 1& Table S1). Peak viscosity during pasting is controlled by the extent of granule swelling, amylose leaching and by the rate of the disruption of the swollen granules caused by shear (Li et al., 2016). Peak viscosity is achieved when the rate of swelling equals the rate of breakdown of the granules (Kumar & Khatkar, 2017). Possibly TA in WS-TA complexes facilitated both the swelling and the breakdown of the swollen granules. A confirmation of the latter may be the higher breakdown viscosity caused by bound TA (Table S1).

Based on DSC and XRD results, we suggest that the addition of TA to WS by complexation or by mixing resulted in the formation of inclusion and non-inclusion complexes. XRD is a direct method to identify V-type inclusion complexes by the appearance of characteristic diffraction peaks at around 7°, 13°, and 20° as reported, for instance, for potato amylose-proanthocyanins, rice starch-gallic acid and corn starch-soy isoflavone inclusion complexes (Amoako & Awika, 2016; Liu, Yuan, et al., 2019; Wang et al., 2020). In our study, the peak at 2θ of 20° was detected in all the samples, including native starch (Fig. 2), which was previously related to the amylose-lipid complex (Liu, Sun, Hou, & Dong, 2016; Maphalla & Emmambux, 2015; Zhang et al., 2012). Therefore, the formation of a V-type starch-tannic acid inclusion complex may not be

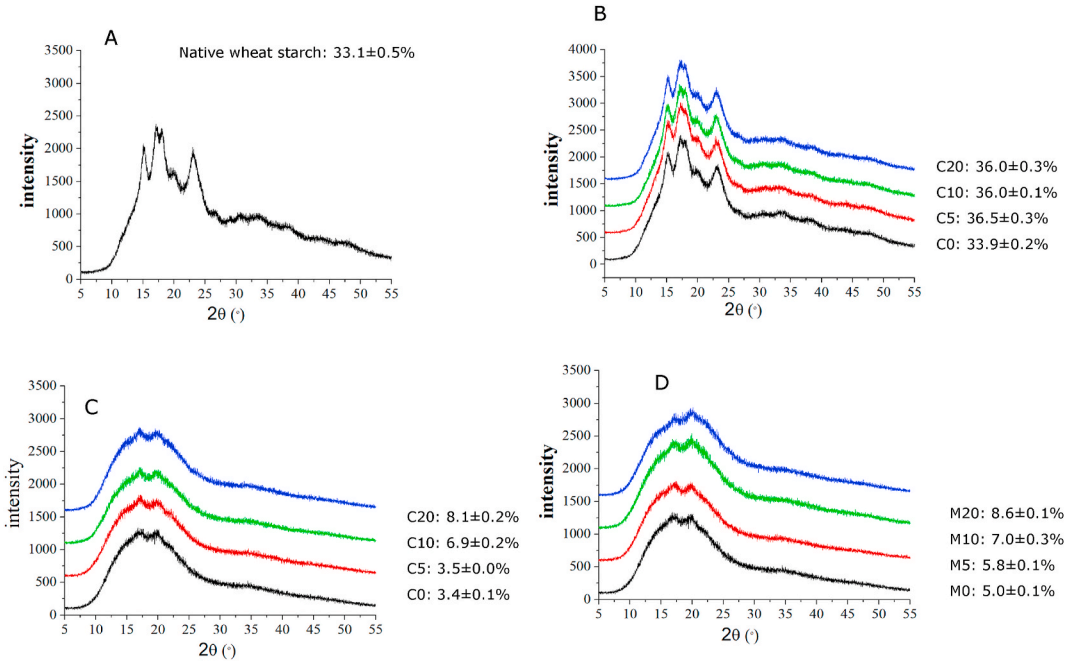


**Fig. 2.** XRD patterns and relative crystallinity of A) Native wheat starch, B) wheat starch-tannic acid complex, C) gelatinized wheat starch-tannic acid complex, D) gelatinized wheat starch-tannic acid mixtures. Relative crystallinity of each samples was marked on the curve. C0, C5, C10 and C20 is the starch-TA complex produced by adding 0%, 5%, 10% and 20% w/w TA to starch and removing the free TA. M5, M10 and M20 were starch-tannins mixtures in this study, which were prepared by simply mixing native starch with 5%, 10% and 20% of tannic acid (dry weight basis of starch). M0 represents NWS (native wheat starch).

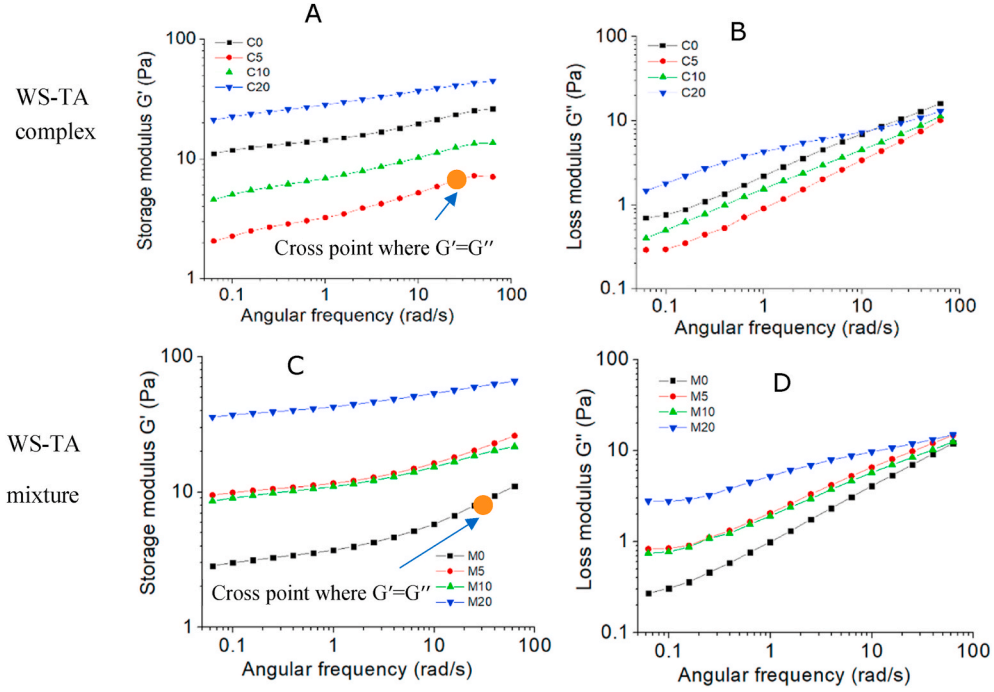


**Fig. 3.** Frequency dependence of (A) Storage modulus (G′) and (B) Loss modulus (G′′) for the WS-TA complex; Frequency dependence of (C) Storage modulus (G′) and (D) Loss modulus (G′) for the WS-TA mixtures. WS, wheat starch; TA, tannic acid. C0, C5, C10 and C20 is the starch-TA complex produced by adding 0%, 5%, 10% and 20% w/w TA to starch and removing the free TA. M5, M10 and M20 were starch-tannins mixtures in this study, which were prepared by simply mixing native starch with 5%, 10% and 20% of tannic acid (dry weight basis of starch). M0 represents NWS (native wheat starch).

distinguished solely by the formation of new peaks. However, we did observe that the peak at 20° become wider in presence of TA (Fig. 2C&D) which may be an indication that starch-tannic acid inclusion complexes may have formed. Similarly, maize starch-caffeic acid inclusion complexes were also identified by increasing intensity of the diffraction peak at 20° (Han et al., 2020), which supports our findings. It is important to mention that the classical mechanism of intrahelical V-amylose complex formation involves the inclusion of a complexing agent in the hydrophobic helical channel of single amylose strands. Some researchers reported that CH-π bonds between starch pyranose rings and phenolic aromatic residues may lead to "V-type amylose" formation (Li, Ndiaye, Corbin, Foegeding, & Ferruzzi, 2020). In this respect, the formation of a classical intrahelical V-amylose complex between WS and TA would not be facilitated by the bulky nature of tannic acid. However, sorghum proanthocyanins, also a bulky molecule, was reported to form inclusion complexes with potato amylose. The proposed mechanism indicated that the hydrophobic core of an amylose coil would include only part of the flavonoid rings (Amoako & Awika, 2016). This may be the case also

**Table 3**
The parameters of the power-law model determined by frequency sweep tests and parameters in the LVE region determined by amplitude sweep tests for wheat starch gel in presence of tannic acid.

| | Frequency sweep tests $G' = k'(\omega)^{n'}$ | | | Amplitude sweep test | |
|---|---|---|---|---|---|
| | $k'$ | $n'$ | $R^2$ | $G'_{LVE}$ (Pa) | tan ($\delta_{LVE}$) |
| C0 | 16.2 ± 1.2 d | 0.11 ± 0.02 bc | 0.98 ± 0.01 | 24.3 ± 0.3 f | 0.26 ± 0.00 b |
| C5 | 4.2 ± 0.8 a | 0.17 ± 0.02 e | 0.97 ± 0.02 | 7.4 ± 0.2 b | 0.41 ± 0.01 e |
| C10 | 8.2 ± 1.1 b | 0.15 ± 0.01 de | 0.99 ± 0.00 | 13.0 ± 0.0 c | 0.31 ± 0.00 d |
| C20 | 26.8 ± 1.8 e | 0.11 ± 0.00 bc | 1.00 ± 0.00 | 41.2 ± 0.2 g | 0.17 ± 0.00 a |
| M0 | 4.3 ± 0.4 a | 0.13 ± 0.01 cd | 0.98 ± 0.01 | 6.4 ± 0.1 a | 0.49 ± 0.02 f |
| M5 | 12.5 ± 0.8 c | 0.08 ± 0.00 a | 0.99 ± 0.00 | 16.2 ± 0.2 d | 0.32 ± 0.01 d |
| M10 | 11.5 ± 0.8 c | 0.10 ± 0.00 b | 0.99 ± 0.01 | 17.1 ± 0.1 e | 0.29 ± 0.01 c |
| M20 | 41.8 ± 1.7 f | 0.07 ± 0.00 a | 0.99 ± 0.00 | 52.6 ± 0.6 h | 0.17 ± 0.00 a |

The power-law model was applied to frequency sweep tests were $G' > G''$. The parameter $k'$ is power-law model constants. The parameter $n'$ is the slope in a log–log plot of $G'$ and $G''$ versus oscillation frequency $w$. tan ($\delta_{LVE}$) = $G''_{LVE}/G'_{LVE}$, $G'_{LVE}$ and $G''_{LVE}$ - storage modulus and loss modulus. C0, C5, C10 and C20 is the starch-TA complex produced by adding 0%, 5%, 10% and 20% w/w TA to starch and removing the free TA. M5, M10 and M20 were starch-tannins mixtures in this study, which were prepared by simply mixing native starch with 5%, 10% and 20% of tannic acid (dry weight basis of starch). M0 represents NWS (native wheat starch). Results are expressed as mean ± standard deviation of triplicate. Different letters in the same column indicate significant difference.

with the TA-starch complexes in our study.

DSC is an indirect method to study interactions between starch and phenolics. The significant increase of the melting enthalpy and of the temperature range ($T_{peak}$ - $T_{onset}$) of the second endothermic transition i.e., amylose-lipid complex (Table 2) further suggested the formation of starch-tannic acid inclusion complexes. The increase in melting enthalpy of amylose-lipid complexes was significantly higher in WS-TA complexes than in the mixtures (Table 2), despite the lower amount of TA present in the complexes (Table 1). Therefore, V-type inclusion complexes would be favoured in WS-TA complexes compared to WS-TA mixtures. In addition, TA may hamper the interaction between lipids and amylose helix (Chao, Yu, Wang, Copeland, & Wang, 2018), thus causing lower dissociation temperatures of amylose-lipid complex (Table 2). The same mechanism may explain the decreased enthalpy of the amylose-lipid related endotherm of WS-TA complexes after re-scan (Table S2). The evidence for the formation of non-inclusion WS-TA was the appearance of a third endothermic transition in DSC results, which was observed at 130–150 °C (Table 2 and Fig. 1). As shown in Fig. 6C, a larger amount of non-inclusion complexes were formed in WS-TA mixtures compared to WS-TA complexes for similar ranges of TA. The endothermic transition associated with these non-inclusion complexes was not thermo-reversible since it did not appear after rescanning (Fig. 1B&D). We suggest that these non-inclusion complex were of amorphous nature and formed mostly through hydrogen bonds (Zhu, 2015).

The sum of the enthalpies associated to inclusion and non-inclusion complexes was significantly correlated to the amount of TA over starch (Fig. 6A), thus suggesting that the interaction with starch was dependent on TA concentration (Chao et al., 2018). However, the contribution to the total enthalpy by inclusion and non-inclusion complexes and the effect of TA concentration was clearly dependent on the method of preparation (Fig. 6B and C). Inclusion complexes were favoured in WS-TA complexes and only beyond a critical amount of TA, i.e. 2% over starch, non-inclusion complexes were formed. Hence, an effective TA concentration for forming non-inclusion complexes in the WS-TA complexes was estimated as the difference between the total TA concentration and the critical amount of 2%. On the contrary, the TA added in the WS-TA mixture was predominantly involved in non-inclusion complexes. As shown in Fig. 6D, the melting enthalpy of the 3rd peak was positively correlated with such an effective amount of TA available to form non-inclusion complexes. Based on these results, we can suggest that these non-inclusion complexes were formed based on similar mechanisms of interaction regardless of the preparation method. On the contrary, the preparation method determined whether inclusion or non-inclusion complexes were favoured in the mechanisms of TA-starch

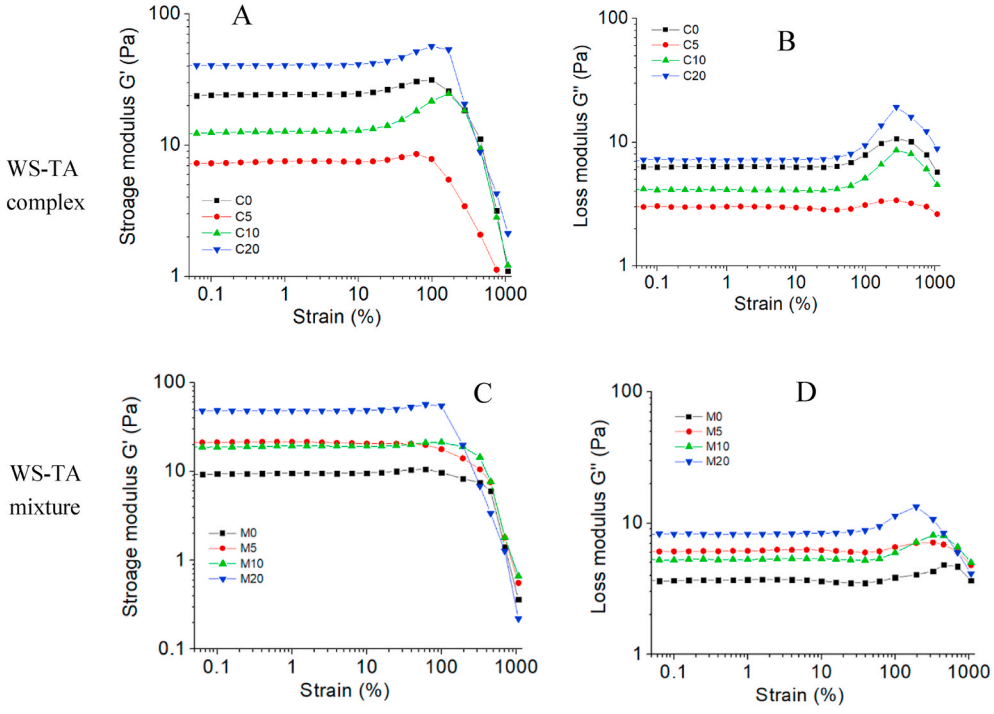


**Fig. 4.** Amplitude dependence of (A) Storage modulus (G′) and (B) Loss modulus (G′′) for the WS-TA complex; Amplitude dependence of (C) Storage modulus (G′) and (D) Loss modulus (G′′) for the WS-TA mixtures. WS, wheat starch; TA, tannic acid. WS-TA0, WS-TA1, WS-TA2 and WS-TA3 were starch-tannins complexes. C0, C5, C10 and C20 is the starch-TA complex produced by adding 0%, 5%, 10% and 20% w/w TA to starch and removing the free TA. M5, M10 and M20 were starch-tannins mixtures in this study, which were prepared by simply mixing native starch with 5%, 10% and 20% of tannic acid (dry weight basis of starch). M0 represents NWS (native wheat starch).

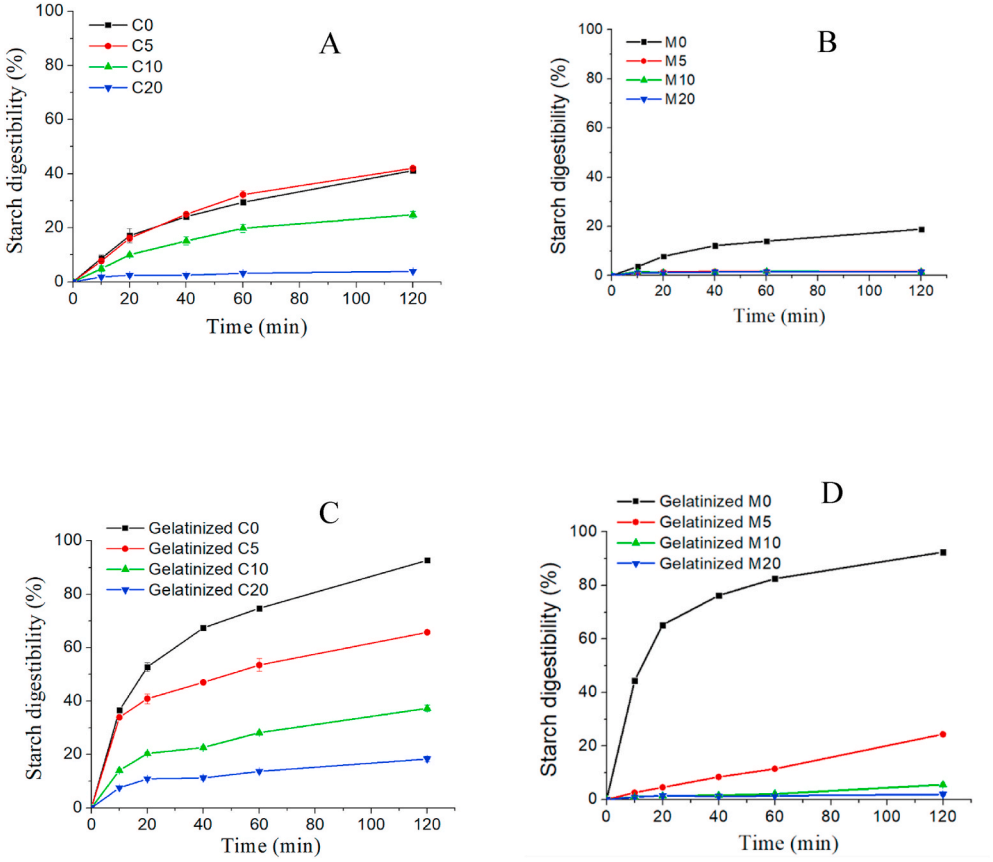


**Fig. 5.** *In vitro* starch hydrolysis profiles of A) non-gelatinized wheat starch-tannic acid complex; B) non-gelatinized wheat starch-tannic acid mixture; C) gelatinized wheat starch-tannic acid complex; D) gelatinized wheat starch-tannic acid mixture. C0, C5, C10 and C20 is the starch-TA complex produced by adding 0%, 5%, 10% and 20% w/w TA to starch and removing the free TA. M5, M10 and M20 were starch-tannins mixtures in this study, which were prepared by simply mixing native starch with 5%, 10% and 20% of tannic acid (dry weight basis of starch). M0 represents NWS (native wheat starch).

**Table 4**
Estimated kinetic parameters for starch digestion obtained from *in vitro* digestion and resistant starch content and bio-accessibility of TA after gastric phase digestion of A) non-gelatinized starch-tannic acid complex; B) mixture of native starch and tannic acid; C) gelatinized starch-tannic acid complex; D) gelatinized mixture of starch and tannic acid.

| Samples A | C0 | C5 | C10 | C20 | Samples B | M0 | M5 | M10 | M20 |
|---|---|---|---|---|---|---|---|---|---|
| k (min-1) | 0.02 ± 0.00 | 0.02 ± 0.00 | 0.02 ± 0.00 | 0.06 ± 0.01 | k ($min^{-1}$) | 0.02 ± 0.00 | NA | NA | NA |
| $C_\infty$ (%) | 44.0 ± 0.0 e | 46.2 ± 0.0 d | 26.9 ± 1.0 c | 3.4 ± 0.1 a | $C_\infty$ (%) | 19.9 ± 0.9 b | NA | NA | NA |
| % * min-1 | 0.9 ± 0.0 | 0.9 ± 0.1 | 0.6 ± 0.1 | 0.2 ± 0.0 | % * $min^{-1}$ | 0.5 ± 0.0 | NA | NA | NA |
| Sum of square | 18.4 ± 15.3 | 2.1 ± 0.7 | 2.2 ± 1.7 | 0.8 ± 0.3 | Sum of square | 2.2 ± 0.5 | NA | NA | NA |
| RS (%) | 1.73 ± 0.02 b | 73.2 ± 0.5 c | 81.6 ± 0.8 d | 83.3 ± 0.9 e | RS (%) | 0.84 ± 0.00 a | NA | NA | NA |
| Bio-accessibility | NA | 0.35 ± 0.02 | 0.47 ± 0.01 | 0.66 ± 0.01 | Bio-accessibility | NA | 3.27 ± 0.50 | 7.68 ± 0.74 | 18.66 ± 0.51 |
| Samples C | Gelatinized C0 | Gelatinized C5 | Gelatinized C10 | Gelatinized C20 | Samples D | Gelatinized M0 | Gelatinized M5 | Gelatinized M10 | Gelatinized M20 |
| k ($min^{-1}$) | 0.04 ± 0.00 | 0.07 ± 0.00 | 0.04 ± 0.00 | 0.06 ± 0.00 | k ($min^{-1}$) | 0.06 ± 0.01 | NA | NA | NA |
| $C_\infty$ (%) | 87.0 ± 0.3 | 58.0 ± 1.1 | 34.9 ± 0.7 | 15.1 ± 0.0 | $C_\infty$ (%) | 87.0 ± 0.3 | NA | NA | NA |
| % * $min^{-1}$ | 3.8 ± 0.2 c | 3.8 ± 0.2 c | 1.2 ± 0.0 b | 1.0 ± 0.0 a | % * $min^{-1}$ | 4.9 ± 0.9 d | NA | NA | NA |
| Sum of square | 130.3 ± 6.0 | 159.1 ± 12.7 | 50.8 ± 11.2 | 11.2 ± 0.0 | Sum of square | 207.9 ± 150.7 | NA | NA | NA |
| RS (%) | 6.5 ± 0.05 b | 42.1 ± 0.1 c | 43.1 ± 0.3 d | 46.5 ± 0.2 e | RS (%) | 5.9 ± 0.0 a | 47.3 ± 0.2f | 49.4 ± 0.3 g | 61.9 ± 0.3 h |
| Bio-accessibility | NA | 0.21 ± 0.01 | 0.19 ± 0.03 | 0.43 ± 0.03 | Bio-accessibility | NA | 1.03 ± 0.03 | 2.59 ± 0.54 | 5.53 ± 0.55 |

C0, C5, C10 and C20 is the starch-TA complex produced by adding 0%, 5%, 10% and 20% w/w TA to starch and removing the free TA. M5, M10 and M20 were starch-tannins mixtures in this study, which were prepared by simply mixing native starch with 5%, 10% and 20% of tannic acid (dry weight basis of starch). M0 represents NWS (native wheat starch). RS, resistant starch. NA, not applicable, it is not applicable because the limited exponential model could not be fitted to the experimental data. The values were expressed as mean ± standard deviation. The values followed by different letters in the same row of $C_\infty$ and RS values indicate significantly different ($p < 0.05$).

interaction.

Both complexed and mixed TA influenced gelatinization of WS. A reduction in the peak temperature of gelatinization $T_{peak}$ was observed in both complex and mixture samples (Table 2). C0 and M0 had significantly different gelatinization temperatures (Table 2), due to the structural re-organization induced by the incubation procedure (Donald, 2001; Renzetti et al., 2021). Therefore, $T_{peak}/T_{peak0}$, instead of $T_{peak}$, was plotted against the actual amount of TA over WS to show the relation between the amount of TA and the gelatinization temperatures (Fig. 6E). A TA-dose dependent reduction of $T_{peak}/T_{peak0}$ (Fig. 6E) was observed. The $T_{peak}$ of starch gelatinization is function of the volume fraction of water available to plasticize the amorphous regions in the

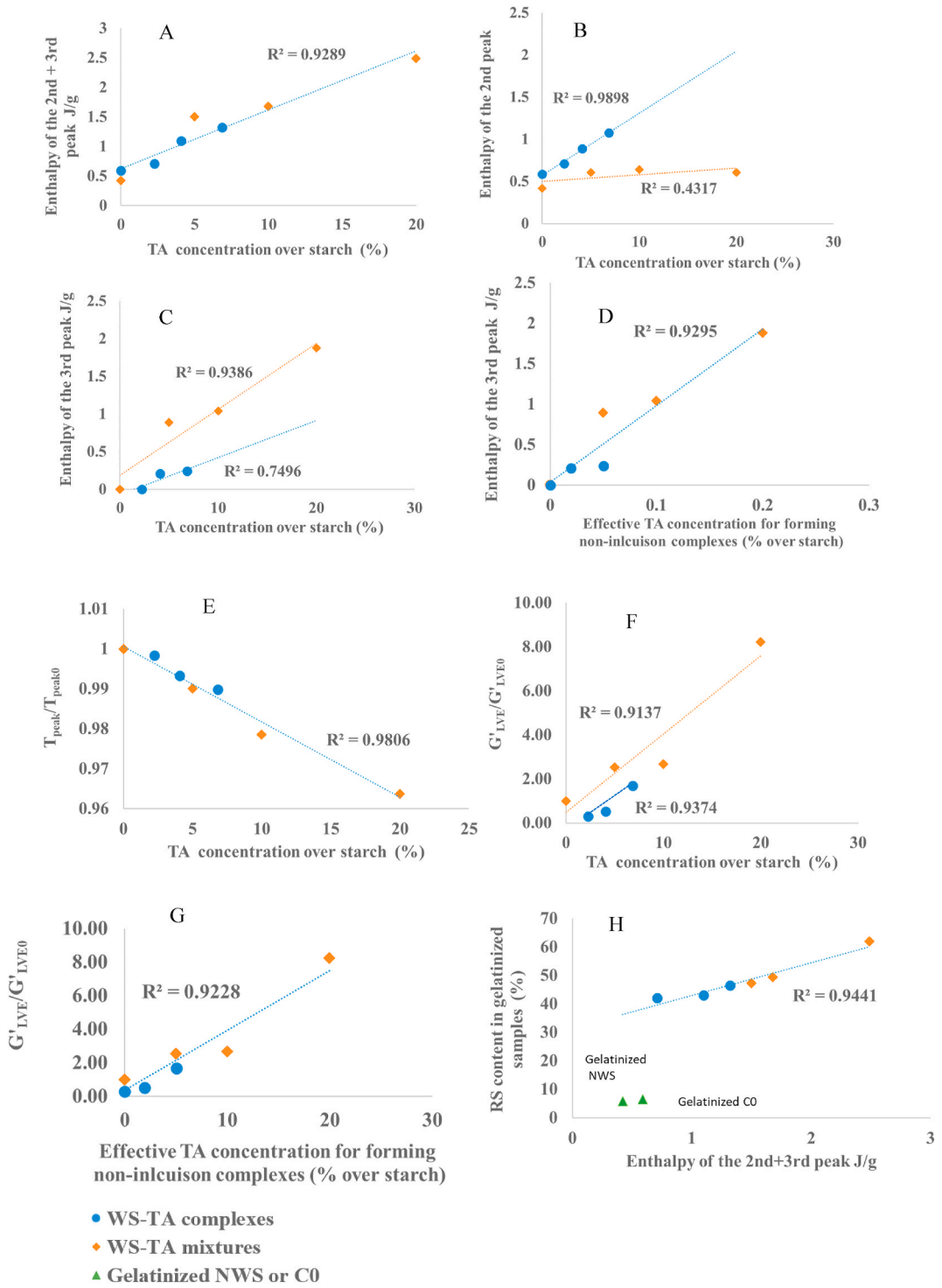


**Fig. 6.** Plots of (A) enthalpy of the 2nd and 3rd peak against TA concentration over starch, (B) enthalpy of the 2nd against TA concentration over starch, (C) enthalpy of the 3rd peak against TA concentration over starch, (D) enthalpy of the 3rd peak against effective TA concentration for forming non-inclusion complexes, (E) $T_{peak}/T_{peak0}$ against TA concentration, (F) $G'_{LVE}/G'_{LVE,0}$ against effective TA concentration for forming non-inclusion complexes, (G) $G'_{LVE}/G'_{LVE,0}$ against TA concentration, (H) Resistant starch content against enthalpy of the 2nd and 3rd peak. Blue represents WS-TA complexes, and orange represents WS-TA mixtures. The data for plotting was from Tables 2 and 3 &4. Regarding WS-TA complexes, $T_{peak0}$ and $G'_{LVE,0}$ are the gelatinized temperature and storage moduli of complex control (C0), respectively. Regarding WS-TA mixtures, $T_{peak0}$ and $G_{LVE,0}$ are the gelatinized temperature and storage moduli of native wheat starch (NWS), respectively. (For interpretation of the references to color in this figure legend, the reader is referred to the Web version of this article.)

starch granule (Donald, 2001; Renzetti et al., 2021). For the WS-TA complexes, the reduction in $T_{peak}$ could be well explained by the decreasing starch concentration. On contrary, for the WS-TA mixtures the starch:water ratio increased as function of increasing TA concentration and an increase in $T_{peak}$ would be expected. It is reasonable to suggest that TA had some plasticizing ability, thus increasing the amount of solvent available for starch gelatinization and thus reducing $T_{peak}$ (Renzetti et al., 2021). In addition, the acidic pH caused by TA should be considered as well. The pH values of the complexes and mixtures was 4.2–4.7, and 3.4–3.6, respectively. A remarkable pH

sensitivity of starch gelatinization was reported and partial hydrolysis of the starch in acidic solutions lowered gelatinization temperature of amylopectin (Builders, Mbah, Adama, & Audu, 2014). The increase in the temperature range of gelatinization, i.e. $T_{peak}$-$T_{onset}$, in both complexes and mixtures (Table 2) implied that the crystallites of starches became heterogeneous due to the addition of TA (Xiao et al., 2011). Green tea polyphenols were also reported to increase the temperature range of gelatinization of rice starch (Xiao et al., 2011). Interestingly, an increase in gelatinization enthalpy was observed in WS-TA complexes (despite not significant), while a significant decrease was observed in the WS-TA mixtures. These results suggest that the method of TA addition, and not the pH, largely affected the mode of interaction with starch, while the TA concentration modulated the size of the observed effects.

During cooling, a starch gel with three-dimensional network can be formed due to the re-arrangement of starch molecules, which can be studied by means of its dynamic viscoelastic properties (Yousefi & Razavi, 2015). All the tested samples showed a weak gel behaviour (Pourfarzad, Yousefi, & Ako, 2021), with the magnitude of $G'$ and $G''$ increasing with an increase in frequency (Fig. 3). The method of addition of TA largely determined the effect of TA concentration on $G'$ and $G''$ (Figs. 3 and 4 &S2). These differences could be well explained by the different amount of inclusion and non-inclusion complexes in WS-TA complexes and mixtures. In the mixtures, a substantial amount of non-inclusion complexes were formed driven by hydrogen bond interactions. These complexes may act as cross-links (i.e. physical junctions), enhancing the elastic behaviour of the heat-set gels (Walstra, 2002). Therefore, increasing TA concentration increased the amount of cross-links, which resulted in the observed increase in $G'$ and $G''$, and in the reduction of frequency dependency, i.e. the $n$ parameter from power-law model (Fig. 3, Table 3). Similar cross-links were also found in amylose-tea polyphenol complexes (Zhu, 2015). The reduction in the $n$ parameter evidenced the formation of a stronger gel network structures in presence of mixed TA compared to the control M0. The cross-linking effect of non-inclusion complexes could be further supported by plotting $G'_{LVE}/G'_{LVE,0}$ against the effective TA concentration available to form non-inclusion complexes (Fig. 6G); where $G'_{LVE,0}$ is the elastic modulus of the control sample (i.e. C0 or M0) and $G'_{LVE}$ the elastic modulus of the WS-TA complexes or mixtures. Since, the incubation procedure during complexation affected the properties of the control C0 compared to the native starch M0, the $G'_{LVE}/G'_{LVE,0}$ parameter allows to compare the relative effect of TA on all WS-TA samples. $G'_{LVE}/G'_{LVE,0}$ increased dependently with TA concentration, but for similar concentration ranges the increase was larger for the WS-TA mixtures than the complexes. It has been previously reported that WS and TA can form soluble complexes, insoluble complexes or even aggregates with increasing TA/WS ratio (Wei, Li, & Li, 2019). However, in the WS-TA complexes a substantial amount of inclusion complexes were formed while non-inclusion complexes only formed at high TA amounts (Table 2). The inclusion complexes were driven by hydrophobic binding and did not form cross-links, as suggested by the reduction in the amount of amylose for re-crystallization. Overall, the formation of inclusion complexes reduced G′ and viscosity and increased the frequency dependence of G′ (Figs. 3–5). By plotting $G'_{LVE}/G'_{LVE,0}$ over the effective TA concentration available for the formation of non-inclusion complexes, it is evident that these physical junctions largely controlled the rheology of the starch gels (Fig. 6G).

In our previous study (Kan, Capuano, et al., 2020), we reported that polyphenols inhibit starch digestion by α-amylase inhibition and starch-polyphenols interactions. In this study, we aimed to gain further insights on the effects of inclusion and non-inclusion complexes on starch digestibility. To distinguish between the effect of TA mediated inhibition of α-amylase and of WS-TA interactions on starch digestibility, α-amylase inhibition by free and bound TA was studied first. 2-Chloro-4-nitrophenyl-α-D-maltotrioside was used as substate to rule out the inhibition resulting from bound TA. Bound TA showed no inhibition on α-amylase, whereas free TA was a strong inhibitor ($IC_{50}$ = 0.16 mg/mL). Therefore, we suggest that the inhibitory effects observed on starch digestibility in non-gelatinized WS-TA complexes could be predominantly attributed to inclusion complexes, since free TA was removed during sample preparation (Fig. 5A). On the contrary, the inhibitory effects on starch digestion observed in non-gelatinized WS-TA mixtures could be attributed to α-amylase inhibition due to the substantial amount of free TA present during digestion (Fig. 5B). Regarding the gelatinized samples, the reduced digestibility ($C_\infty$) and the increased RS could be largely related to the formation of the inclusion and non-inclusion complexes with amylose. In fact, a positive relation was observed between the RS values and the sum of the enthalpies from the endothermic transitions (i.e. peak 2 and peak 3 in Table 2) of all the WS-TA samples (Fig. 6H), which accounts for the amount of inclusion and non-inclusion complexes formed. However, inhibition of α-amylase cannot be completely ruled out in gelatinized WS-TA complexes and mixtures due to the presence of free TA that is released during digestion of starch (bio-accessibility data in Table 4) or free TA that has not bound to starch during gelatinization (in the case of mixtures).

In this study, the effects of tannic acid on the physicochemical properties and *in vitro* digestibility of wheat starch were investigated. Tannic acid was added by complexing and simply mixing with wheat starch. We suggest that wheat starch interacted with tannic acid forming both inclusion and non-inclusion complexes. Non-inclusion complexes were better formed during gelatinization from a simple mix with TA than from TA previously associated with ungelatinized starch. On the contrary, inclusion complexes would be formed from TA previously associated with ungelatinized. Non-inclusion complexes acted as physical cross-links in the starch gels and thus induced an increase in G′ and a reduction in the frequency dependency of G′. The inclusion and non-inclusion complexes both inhibited the digestibility of the gelatinized starch. Overall, this study extends the available knowledge for a better understanding of starch–polyphenol interactions and their effects on physicochemical properties of starch and on its digestibility. These insights can provide with new opportunities in the design of healthy starchy food by application of tannic acid.

## CRediT author statement

Lijiao Kan: Conceptualization, Data curation, Formal analysis, Investigation, Methodology, Visualization, Writing - original draft, Writing - review & editing. Edoardo Capuano: Funding acquisition, Conceptualization, Methodology, Supervision, Writing - review & editing, Project administration; Teresa Oliviero: Funding acquisition, Conceptualization, Methodology, Supervision, Writing - review & editing, Project administration; Stefano Renzetti: Conceptualization, Data curation, Methodology, Formal analysis, Visualization, Supervision, Writing - review & editing.

## Declaration of competing InterestCOI

There are no conflicts of interest to declare.

## Acknowledgement

The author Lijiao Kan received a PhD scholarship from the China Scholarship Council (No. 201706820018).

## Appendix A. Supplementary data

Supplementary data to this article can be found online at https://doi.org/10.1016/j.foodhyd.2021.107459.

## References


Amoako, D. B., & Awika, J. M. (2016). Polymeric tannins significantly alter properties and in vitro digestibility of partially gelatinized intact starch granule. *Food Chemistry, 208*, 10–17. https://doi.org/10.1016/j.foodchem.2016.03.096

Biliaderis, C. G., & Galloway, G. (1989). Crystallization behavior of amylose-V complexes: Structure-property relationships. *Carbohydrate Polymers, 71*, 380–387. https://doi.org/10.1016/j.carbpol.2007.06.010

Blazek, J., & Copeland, L. (2008). Pasting and swelling properties of wheat flour and starch in relation to amylose content. *Carbohydrate Polymers, 71*, 380–387. https://doi.org/10.1016/j.carbpol.2007.06.010

Brassinne, J., Gohy, J. F., & Fustin, C. A. (2014). Controlling the cross-linking density of supramolecular hydrogels formed by heterotelechelic associating copolymers. *Macromolecules, 47*, 4514–4524. https://doi.org/10.1021/ma500537t

Builders, P. F., Mbah, C. C., Adama, K. K., & Audu, M. M. (2014). Effect of pH on the physicochemical and binder properties of tigernut starch. *Starch Staerke, 66*, 281–293. https://doi.org/10.1002/star.201300014

Chai, Y., Wang, M., & Zhang, G. (2013). Interaction between amylose and tea polyphenols modulates the postprandial glycemic response to high-amylose maize starch. *Journal of Agricultural and Food Chemistry, 61*, 8608–8615. https://doi.org/10.1021/jf402821r

Chao, C., Yu, J., Wang, S., Copeland, L., & Wang, S. (2018). Mechanisms underlying the formation of complexes between maize starch and lipids. *Journal of Agricultural and Food Chemistry, 66*, 272–278. https://doi.org/10.1021/acs.jafc.7b05025

Chi, C., Li, X., Zhang, Y., Chen, L., Li, L., & Wang, Z. (2017). Digestibility and supramolecular structural changes of maize starch by non-covalent interactions with gallic acid. *Food & Function, 8*, 720–730. https://doi.org/10.1039/c6fo01468b

Donald, A. M. (2001). Plasticization and self assembly in the starch granule. *Cereal Chemistry, 78*, 307–314. https://doi.org/10.1094/CCHEM.2001.78.3.307

Dona, A. C., Pages, G., Gilbert, R. G., & Kuchel, P. W. (2010). Digestion of starch: In vivo and in vitro kinetic models used to characterise oligosaccharide or glucose release. *Carbohydrate Polymers, 80*, 599–617. https://doi.org/10.1016/J.CARBPOL.2010.01.002

Gao, S., Liu, H., Sun, L., Cao, J., Yang, J., Lu, M., et al. (2021). Rheological, thermal and in vitro digestibility properties on complex of plasma modified Tartary buckwheat starches with quercetin. *Food Hydrocolloids, 110*, 106209. https://doi.org/10.1016/j.foodhyd.2020.106209

Guo, Z., Zhao, B., Chen, J., Chen, L., & Zheng, B. (2019). Insight into the characterization and digestion of lotus seed starch-tea polyphenol complexes prepared under high hydrostatic pressure. *Food Chemistry, 297*, 124992. https://doi.org/10.1016/j.foodchem.2019.124992

Han, M., Bao, W., Wu, Y., & Ouyang, J. (2020). Insights into the effects of caffeic acid and amylose on in vitro digestibility of maize starch-caffeic acid complex. *Journal of Biological Macromolecules, 162*, 922–930. https://doi.org/10.1016/j.ijbiomac.2020.06.200

Kan, L., Capuano, E., Fogliano, V., Oliviero, T., & Verkerk, R. (2020). Tea polyphenols as a strategy to control starch digestion in bread: The effects of polyphenol type and gluten. *Food & Function, 11*, 5933–5943. https://doi.org/10.1039/d0fo01145b

Kan, L., Oliviero, T., Verkerk, R., Fogliano, V., & Capuano, E. (2020). Interaction of bread and berry polyphenols affects starch digestibility and polyphenols bio-accessibility. *Journal of Functional Foods, 68*, 103924. https://doi.org/10.1016/j.jff.2020.103924

Kumar, R., & Khatkar, B. S. (2017). Thermal, pasting and morphological properties of starch granules of wheat (Triticum aestivum L.) varieties. *Journal of Food Science & Technology, 54*, 2403–2410. https://doi.org/10.1007/s13197-017-2681-x

Li, H., Dhital, S., Slade, A. J., Yu, W., Gilbert, R. G., & Gidley, M. J. (2019). Altering starch branching enzymes in wheat generates high-amylose starch with novel molecular structure and functional properties. *Food Hydrocolloids, 92*, 51–59. https://doi.org/10.1016/j.foodhyd.2019.01.041

Li, W., Gao, J., Wu, G., Zheng, J., Ouyang, S., Luo, Q., et al. (2016). Physicochemical and structural properties of A- and B-starch isolated from normal and waxy wheat: Effects of lipids removal. *Food Hydrocolloids, 60*, 364–373. https://doi.org/10.1016/j.foodhyd.2016.04.011

Li, M., Ndiaye, C., Corbin, S., Foegeding, E. A., & Ferruzzi, M. G. (2020). Starch-phenolic complexes are built on physical CH-π interactions and can persist after hydrothermal treatments altering hydrodynamic radius and digestibility of model starch-based foods. *Food Chemistry, 308*, 125577. https://doi.org/10.1016/j.foodchem.2019.125577

Li, M., Pernell, C., & Ferruzzi, M. G. (2018). Complexation with phenolic acids affect rheological properties and digestibility of potato starch and maize amylopectin. *Food Hydrocolloids, 77*, 843–852. https://doi.org/10.1016/j.foodhyd.2017.11.028

Liu, Y., Chen, L., Xu, H., Liang, Y., & Zheng, B. (2019). Understanding the digestibility of rice starch-gallic acid complexes formed by high pressure homogenization. *Journal of Biological Macromolecules, 134*, 856–863. https://doi.org/10.1016/j.ijbiomac.2019.05.083

Liu, P., Sun, S., Hou, H., & Dong, H. (2016). Effects of fatty acids with different degree of unsaturation on properties of sweet potato starch-based films. *Food Hydrocolloids, 61*, 351–357. https://doi.org/10.1016/j.foodhyd.2016.05.033

Liu, S., Yuan, T. Z., Wang, X., Reimer, M., Isaak, C., & Ai, Y. (2019). Behaviors of starches evaluated at high heating temperatures using a new model of Rapid Visco Analyzer – RVA 4800. *Food Hydrocolloids, 94*, 217–228. https://doi.org/10.1016/j.foodhyd.2019.03.015

Maphalla, T. G., & Emmambux, M. N. (2015). Functionality of maize, wheat, teff and cassava starches with stearic acid and xanthan gum. *Carbohydrate Polymers, 136*, 970–978. https://doi.org/10.1016/j.carbpol.2015.09.004

Minekus, M., Alminger, M., Alvito, P., Ballance, S., Bohn, T., Bourlieu, C., et al. (2014). A standardised static *in vitro* digestion method suitable for food – an international consensus. *Food & Function, 5*, 1113–1124. https://doi.org/10.1039/C3FO60702J

Okutan, L., Kongstad, K. T., Jäger, A. K., & Staerk, D. (2014). High-resolution α-amylase assay combined with high-performance liquid chromatography-solid-phase extraction-nuclear magnetic resonance spectroscopy for expedited identification of α-amylase inhibitors: Proof of concept and α-amylase inhibitor in cinnamon. *Journal of Agricultural and Food Chemistry, 62*, 11465–11471. https://doi.org/10.1021/jf5047283

Oliviero, T., & Fogliano, V. (2016). Food design strategies to increase vegetable intake: The case of vegetable enriched pasta. *Trends in Food Science & Technology, 51*, 58–64. https://doi.org/10.1016/j.tifs.2016.03.008

Pan, J., Li, M., Zhang, S., Jiang, Y., Lv, Y., Liu, J., et al. (2019). Effect of epigallocatechin gallate on the gelatinisation and retrogradation of wheat starch. *Food Chemistry, 294*, 209–215. https://doi.org/10.1016/j.foodchem.2019.05.048

Pourfarzad, A., Yousefi, A., & Ako, K. (2021). Steady/dynamic rheological characterization and FTIR study on wheat starch-sage seed gum blends. *Food Hydrocolloids, 111*, 106380. https://doi.org/10.1016/j.foodhyd.2020.106380

Renzetti, S., van den Hoek, I. A. F., & van der Sman, R. G. M. (2021). Mechanisms controlling wheat starch gelatinization and pasting behaviour in presence of sugars and sugar replacers: Role of hydrogen bonding and plasticizer molar volume. *Food Hydrocolloids, 119*, 106880. https://doi.org/10.1016/j.foodhyd.2021.106880

Van Hung, P., Phat, N. H., & Phi, N. T. L. (2013). Physicochemical properties and antioxidant capacity of debranched starch-ferulic acid complexes. *Starch Staerke, 65*, 382–389. https://doi.org/10.1002/star.201200168

Waigh, T. A., Gidley, M. J., Komanshek, B. U., & Donald, A. M. (2000). The phase transformations in starch during gelatinisation: A liquid crystalline approach. *Carbohydrate Research, 328*, 165–176. https://doi.org/10.1016/S0008-6215(00)00098-7

Walstra, P. (2002). In (1st ed.)*Soft solidsPhysical chemistry of foods* (Chapter 17)).

Wang, S., Wu, T., Cui, W., Liu, M., Wu, Y., Zhao, C., et al. (2020). Structure and in vitro digestibility on complex of corn starch with soy isoflavone. *Food Sciences and Nutrition, 8*, 6061–6068. https://doi.org/10.1002/fsn3.1896

Wei, X., Li, J., & Li, B. (2019). Multiple steps and critical behaviors of the binding of tannic acid to wheat starch: Effect of the concentration of wheat starch and the mass ratio of tannic acid to wheat starch. *Food Hydrocolloids, 94*, 174–182. https://doi.org/10.1016/j.foodhyd.2019.03.019

Xiao, H., Lin, Q., Liu, G. Q., Wu, Y., Tian, W., Wu, W., et al. (2011). Effect of green tea polyphenols on the gelatinization and retrogradation of rice starches with different amylose contents. *Journal of Medicinal Plants Research, 5*, 4298–4303. https://doi.org/10.5897/JMPR.9000481

Yousefi, A. R., & Razavi, S. M. A. (2015). Dynamic rheological properties of wheat starch gels as affected by chemical modification and concentration. *Starch Staerke, 67*, 567–576. https://doi.org/10.1002/star.201500005

Zhang, B., Huang, Q., Luo, F. xing, & Fu, X. (2012). Structural characterizations and digestibility of debranched high-amylose maize starch complexed with lauric acid. *Food Hydrocolloids, 28*, 174–181. https://doi.org/10.1016/j.foodhyd.2011.12.020

Zhang, B., Li, X., Liu, J., Xie, F., & Chen, L. (2013). Supramolecular structure of A- and B-type granules of wheat starch. *Food Hydrocolloids, 31*, 68–73. https://doi.org/10.1016/j.foodhyd.2012.10.006

Zhao, B., Wang, B., Zheng, B., Chen, L., & Guo, Z. (2019). Effects and mechanism of high-pressure homogenization on the characterization and digestion behavior of lotus seed starch–green tea polyphenol complexes. *Journal of Functional Foods, 57*, 173–181. https://doi.org/10.1016/j.jff.2019.04.016

Zheng, Y., Tian, J., Kong, X., Wu, D., Chen, S., Liu, D., et al. (2021). Proanthocyanidins from Chinese berry leaves modified the physicochemical properties and digestive characteristic of rice starch. *Food Chemistry, 335*, 127666. https://doi.org/10.1016/j.foodchem.2020.127666

Zhu, F. (2015). Interactions between starch and phenolic compound. *Trends in Food Science & Technology, 43*, 129–143. https://doi.org/10.1016/J.TIFS.2015.02.003